Received: 22 November 2016 | Accepted: 28 December 2016

DOI: 10.1111/ijac.12654

ORIGINAL ARTICLE

International Journal of Applied Ceramic TECHNOLOGY

Densification and characterization of rapid carbothermal synthesized boron carbide

Muhammet Fatih Toksoy[1] | William Rafaniello[2] | Kelvin Yu Xie[3] | Luoning Ma[3] | Kevin Jude Hemker[3] | Richard Alan Haber[2]

[1]Mechanical Engineering, Izmir Institute of Technology, Urla, Izmir, Turkey

[2]Materials Sci. & Eng, Rutgers University, New Brunswick, NJ, USA

[3]Mechanical Engineering, Johns Hopkins University, Baltimore, MD, USA

Correspondence
Muhammet Fatih Toksoy and Richard Haber
Emails: fatihtoksoy@iyte.edu.tr; rhaber1@rci.rutgers.edu

Funding information
Army Research Laboratory, Grant/Award Number: W911NF-12-2-0022; Defense Advanced Research Projects Agency, Grant/Award Number: W31P4Q-13-1-0001; National Science Foundation, Grant/Award Number: 1540027

Abstract

Submicrometer boron carbide powders were synthesized using rapid carbothermal reduction (RCR) method. Synthesized boron carbide powders had smaller particle size, lower free carbon, and high density of twins compared to commercial samples. Powders were sintered using spark plasma sintering at different temperatures and dwell times to compare sintering behavior. Synthesized boron carbide powders reached >99% TD at lower temperature and shorter dwell times compared to commercial powders. Improved microhardness observed in the densified RCR samples was likely caused by the combination of higher purity, better stoichiometry control, finer grain size, and a higher density of twin boundaries.

KEYWORDS

boron carbide, spark plasma sintering, synthesis, twinning

1 | INTRODUCTION

Boron carbide is the third hardest material known after diamond and cubic boron nitride. The strength-density ratio is noticeably higher than most materials. Low density and extraordinary hardness values make boron carbide very desirable for extreme environments. Knoop hardness of boron carbide is reported to be 28.5-30.5 GPa with a 100 g indentation load (HK_{100}), and 27.5-28.5 GPa with a 200 g indentation load (HK_{200}).[1–5] Improved strength and hardness of boron carbide can be achieved by reducing porosity and grain size.[6–9] Mechanical properties are also affected by homogeneity, inclusions, and stoichiometry. For example, the hardness of boron carbide peaks at B_4C composition, and decreases as boron content increases.[10,11]

Although possessing extraordinary mechanical properties, producing high-purity boron carbide powder is challenging. The carbothermal reduction method is the conventional approach for synthesizing boron carbide powders. This method is relatively low cost, utilizing inexpensive, readily available raw materials (boric acid and carbon black) and a noncomplex, scalable manufacturing process. The basic principal of this method is the reduction in boron oxide with carbon in an electric arc furnace.[12–15] These results in a large ingot that requires extensive milling to produce micrometer sized ceramic grade powders. Milling typically yields a wide particle size distribution and a relatively high degree of metallic impurities despite the incorporation of a postmilling acid leach step. Unreacted-free carbon is commonly found in the finished boron carbide powder.[16–18] In this work, a nonconventional boron carbide powder synthesis method-rapid carbothermal reduction (RCR) was employed to produce finer and higher purity powders. RCR is a process (Figure 1) that transports precursors into a reactor furnace at the reaction temperature, where vapor phase boron oxide and solid carbon react above 1600°C. Upon entering the hot zone, the precursor reaches the reaction temperature with extreme heating rate (10^3-10^5 K/s). Boron oxide rapidly sublimates and reacts with the intimately mixed carbon source to produce boron carbide. Carbon monoxide and excess boron oxide gases leave the furnace from an exhaust line. Boron oxide loss is

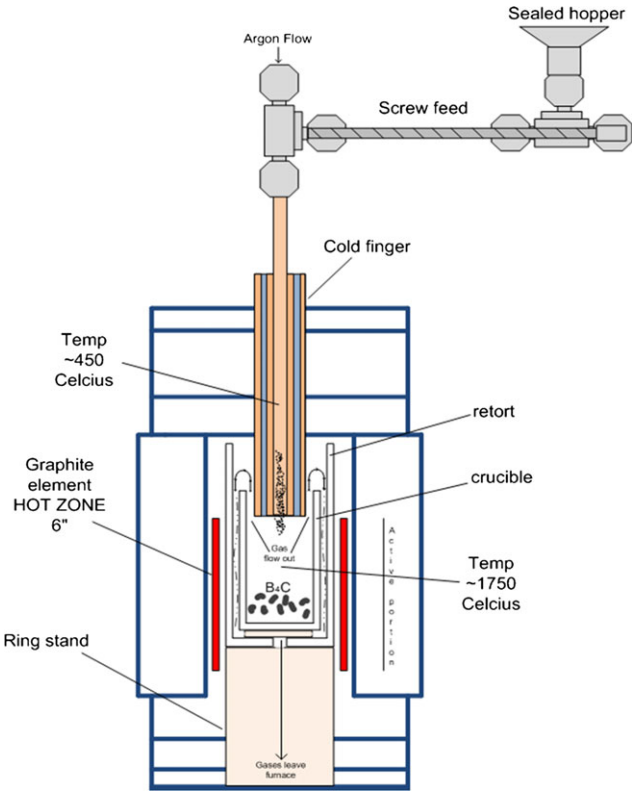

FIGURE 1 Schematic of rapid carbothermal reduction process. [Color figure can be viewed at wileyonlinelibrary.com]

dependent on the reactor temperature, and the precursor composition. This reaction yields submicrometer size, stoichometric boron carbide powder without free carbon.[19–21]

Another challenge that limits the full potential of boron carbide in many applications is the difficulty in sintering. Sintering aids are often used to lower the boron carbide sintering temperature. Carbon, elemental boron, and metallic additives have been used as sintering aids to decrease the sintering temperature and limit grain growth but often with some compromise in mechanical properties.[22–25] Among all the sintering additives, carbon is the main secondary phase found in dense boron carbide. The presence of the carbon secondary phase results in the decrease in mechanical properties for boron carbide.[26–28] Hot pressing is widely used to produce highly dense articles. Boron carbide can be hot pressed to high densities without additives, but only at very high temperature. Full density is often achieved using different combinations of temperature and dwell times that depend on the average particle size. Typical temperatures need to be higher than 2200°C for short dwell times and between 2100 and 2200°C with longer dwell times. Grain growth is inevitable in both scenarios.[29–32] An alternative densification method is spark plasma sintering (SPS). SPS applies pressure and a high electric current directly through graphite dies in contrast to indirect induction or resistive heating used in hot pressing. This electric current creates hot spots at particle contact points and generates extreme heating at particle surfaces, which facilitates the densification. Neck formation and diffusion start at a very early stage of the sintering cycle and allow densification to proceed at considerably lower temperatures.[33–37] Due to high heating rates and relatively short dwell times from SPS, grain growth is limited. SPS has been successfully applied to densify commercial boron carbide powders without sintering additives, and the reported sintering temperatures are well below those in hot pressing. Densities of 98% theoretical density (TD) were achieved near 1600°C, whereas full density was achieved at temperatures as low as 1700°C, with limited grain growth. These samples exhibit enhanced mechanical properties compared to traditionally sintered boron carbide pieces as a result of limited grain growth with high density. Because of differences in sample size and temperature measurement techniques comparing SPS experiments are challenging given the uncertainty in the true temperature of the sample.[38–42] However, while direct temperature comparisons may not be possible, density and microstructure features are readily discernible.

In this work, boron carbide powders were fabricated with higher purity and smaller boron average particle size using RCR synthesis technique. In addition, an unexpected presence of high density of growth twins were observed in all powder particles, which is largely absent in commercial powders. Furthermore, these RCR boron carbide powders were densified to near theoretical density using SPS. The dense RCR boron carbide samples were generated at lower temperature with shorter dwell times compared to the densification behavior of the evacuated commercial powders. The dense RCR boron carbide also retained many twins, which may be the cause of an observed higher hardness compared with dense, twin-free boron carbide bodies produced using the commercial powders.

2 | EXPERIMENTAL PROCEDURE

Boric acid (US-Borax) was dissolved in a beaker with deionized (DI) water at 80°C, whereas in a separate beaker the carbon source (Cabot Vulcan X-72, Fischer Lamp Black) was dispersed in DI water and addition of surfactant (Triton X-100). Carbon slurry was slowly poured into boric acid slurry and stirred for 30 minutes. Then the mixture was heated further to evaporate most of water to form a carbon-boric acid paste which is then placed into drying oven and dried (for at least twelve hours) between 120 and 140°C. Dried product was placed into an electric tube furnace and calcined at 600°C under constant argon flow. Calcined chunks were placed into a mortar and crushed and only particles between 125 and 425 μm were used for

RCR feeding. Precursor was put into the sealed hopper and furnace (RCR is shown in Figure 1) was heated to the 1825°C and precursor was kept in the hopper until the furnace temperature stabilized. Feeder system was turned on to feed materials with 1.5 g/min feeding rate. Precursor travels from hopper to cold finger using screw feeder. Precursor was kept cool as it fell through cold finger into the furnace. Reacted powder accumulated in the crucible and the produced gas byproducts left the system through the exhaust line. Two boron carbide powders were synthesized by using two different carbon sources, lampblack (Fisher Scientific) and Vulcan XC-72 (Cabot Specialty Carbon Black). Vulcan XC-72 or Vulcan (80-235 m^2/g) has larger surface area compared to lampblack carbon (22-90 m^2/g). These powders were labeled as R-SF9 and R-SF10, respectively.

Carbon analyses (LECO CS-230), oxygen analyses (LECO TC-600), and boron titration (ASTM C-791) analyses were completed for every boron carbide powder. X-ray diffractometry (PANanalytical X'Pert) was used for phase identification and recorded files were analyzed using the analysis software (MDI Jade). Boron carbide, elemental boron, boron oxide species, and carbon was targeted for matching the peaks. Rietveld analyses for lattice measurements were completed after peak match. Aselage et al. demonstrated there is a relationship between lattice parameters and stoichiometry. Stoichiometry of boron carbide was determined from lattice parameters and converted to wt% carbon (20 at.% carbon corresponds to 21.7 wt%). Free carbon was calculated by subtracting bound carbon (calculated from stoichiometry) from total carbon from carbon analysis. Existed nitrogen and oxygen were considered as bounded to boron and taken to consideration for free carbon estimation.[43,44] FESEM (Zeiss-Sigma) analysis was performed to analyze powder morphology and characterization. These analysis were performed for two commercial powders (H.C. Starck, Grade HD20 and UK Abrasives F1500) and results were compared between commercial and RCR synthesized powders.

To achieve dense boron carbide samples, powders were densified with SPS furnace (Thermal Technology 10 Series) under argon atmosphere with 50 MPa applied pressure and a heating ramp rate of 300°C/min. To produce similar size samples, approximately four grams of powders were placed into 20 mm diameter graphite die. Temperature measurements were taken from a hole on the side of the die using high-temperature pyrometer. Sintering temperatures of 1550°C, 1700°C, 1850°C, and 1900°C were studied without dwell and additional samples were prepared with 5-, 10-, and 20-minute dwell times at 1900°C.

Densities of sintered samples were determined using Archimedes immersion testing. Samples were cut along cross sections and polished to an optical finish. Knoop microhardness was taken at 100, 300, 500, and 1000 g loads with 10 measurements for each load (Leco M400 Microhardness Tester). Samples were etched by electrolytic method using 0.1% KOH solution and 5 V applied for approximately 1 minute. Grain size measurements were taken from linear intercept analyses from the FESEM images using computer software Lince (by Technische Universität Darmstadt). To prepare TEM specimens, the powders were suspended in ethanol and then dispersed on holey carbon supporting films. Dense samples were sliced using a low speed diamond saw, polished using diamond lapping films to form wedge-shaped specimens, and then further thinned to electron transparency using an ion mill at 4 kV and 1 mA. TEM observations were conducted in a Phillips CM300 field-emission transmission electron microscope operating at 300 kV, to observe microstructural features such as porosity, grain size, and the presence of twins.

3 | RESULTS AND DISCUSSIONS

3.1 | Powder synthesis and characterization

Submicrometer equiaxed boron carbide powders were synthesized with reduced free carbon using RCR synthesis method. Figure 2 shows the morphologies of boron carbide powders used in this study. Carbon sources affected morphology and particle size differently. Lampblack containing precursors resulted in larger (d_{90}: 0.90 μm) boron carbide powder (R-SF9), whereas precursors with Vulcan carbon yielded much smaller (d_{90}: 0.45 μm) particles (R-SF10). Carbon source with larger surface area yielded smaller reacted particles likely due to the more intimate mixing of the boron oxide with the Vulcan carbon. The commercial UK boron carbide powder had a wider particle size distribution, characterized by angular morphology characteristic of milled (fractured) particles. Morphology of Starck boron carbide powder was less angular than the UK powder and average particle size was much smaller. However, there were also larger particles (up to 5 μm) observed in the Starck powder.

Boron carbide powders were analyzed and characterized by several characterization methods. B/C ratios (stoichiometry) varied between 4.04-4.45 and complete characterization results are shown in Table 1. Synthesized powders, R-SF9 and R-SF10, had relatively low-free carbon content (0.40 and 0.10 wt%, respectively). Homogenously distributed free carbon, as high 2.5 wt%, was present in UK powder. Starck powder had 1.0% free carbon that was in the form of agglomerates.

The particle size and morphology measurement from TEM agrees well with the SEM observations (Figure 3).

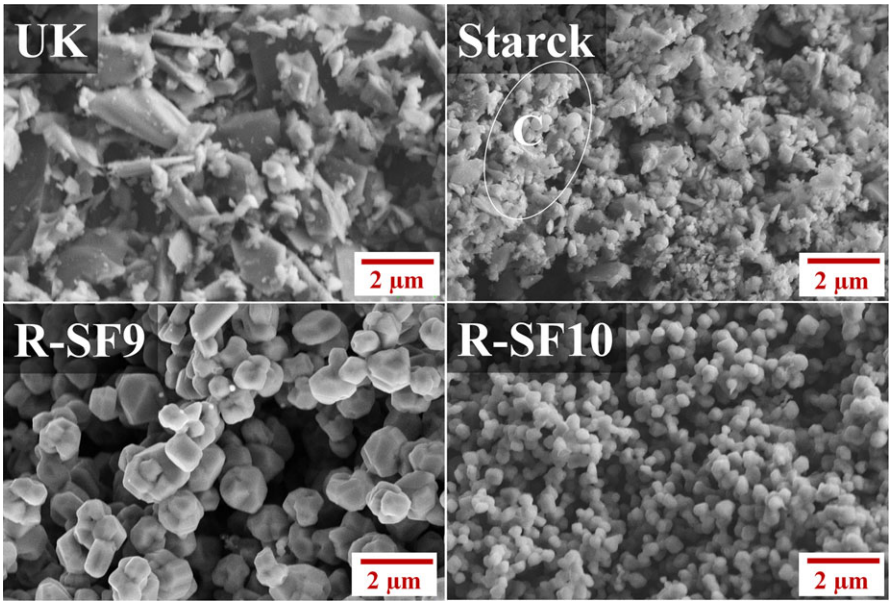

FIGURE 2 SEM images of boron carbide powders, carbon agglomeration is shown with encircled C sign. [Color figure can be viewed at wileyonlinelibrary.com]

TABLE 1 Properties of boron carbide powders

Name	d_{10} (μm)	d_{50} (μm)	d_{90} (μm)	Free C (%)	Carbon (%)	Oxygen (%)	Nitrogen (%)	Boron (%)	B/C ratio
R-SF9	0.20	0.50	0.90	0.40	21.15	0.44	0.16	77.87	4.17
R-SF10	0.10	0.20	0.45	0.10	20.50	0.47	0.01	78.93	4.28
UK	0.30	1.27	2.60	2.50	20.98	3.61	0.04	75.61	4.41
Starck	0.10	0.50	0.85	1.00	22.16	1.58	0.20	76.00	4.04

The RCR powder particles had equiaxed morphology, were submicrometer in size and only a limited number of larger particles were observed. On the other hand, UK powder showed heterogeneous particle size and morphology. Each particle had different shape. Starck powder was observed to be more homogenous compared to UK powder, but still less uniform compared to the RCR powders. In addition, HRTEM also revealed the microstructural features within the particles. All RCR particles were observed to contain high density of twins (two examples are shown in Figure 4). Generally speaking, the smaller the particle, higher the twin density. The twins were observed only a few nanometers apart in the small particles (~200 nm) and tens of nanometers apart in larger particles (~800 nm). In contrast, most of the particles in the commercial powders were observed to be free of twins. Twins were observed within only a few particles of UK powder as indicated in Figure 3 and HRTEM observations of commercial powders showed no sign of twin. TEM and HRTEM analyses (Figure 4) revealed twins are very limited in commercial boron carbide powders. Due to nature of RCR process, extremely rapid reaction occurs in high temperatures and reaction is completed in the order of milliseconds. Thus boron carbide layers are nucleated in the preferred direction, results the high twin density. Heating rate is highly depended on precursor size which also affects the final particle size. Smaller particles were results of faster synthesis so twin density is higher. Thus R-SF10 has smaller particle size and higher twin density. Also Xie et al. showed that twin existence is highly depended on the stoichiometry and structural hierarchy,[45] thus controlling the boron carbide stoichiometry also play important role on twin density.

3.2 | Densification

Densities of the samples were measured with Archimedes methods and results are summarized in Table 2. RCR boron carbide samples and Starck samples initially had lower density than the UK sample at 1550°C due to their lower initial packing density compared to UK. However, density of RCR boron carbide samples was higher than the commercial boron carbide samples at 1700°C, shown by density curves in Figure 5. RCR boron carbide samples and Starck sample had steep densification rate up to 1850°C. This rate decreased dramatically as full densification was approached.

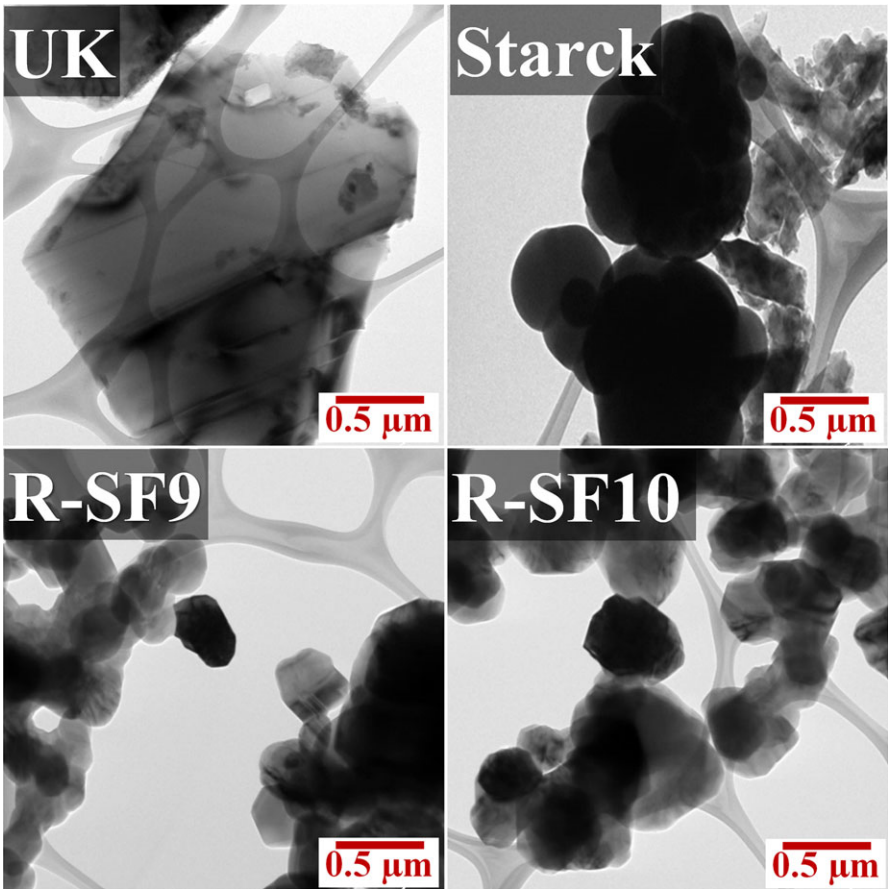

FIGURE 3 TEM images of boron carbide powders. [Color figure can be viewed at wileyonlinelibrary.com]

To gain further insight on the densification process of all the boron carbide powders, the powders were processed starting at 1550°C, 1700°C, 1850°C, and 1900°C to investigate the onset of sintering. Figure 6 shows particle rearrangement, surface smoothening and limited neck formation at this 1550°C. Neck formation was observed in every sample. Boron carbide samples at this temperature demonstrated characteristics of initial stage of sintering. Necking was more apparent for every particle in all the samples at 1700°C and densities of R-SF9 and R-SF10 surpassed the density of boron carbide samples from commercial powders. R-SF9 and R-SF10 had higher measured density as reflected by the microstructural features (Figure 7). Only limited number of small (0.20-0.50 μm) pores was observed throughout R-SF9 and R-SF10 samples. Densification of commercial powders under the same condition was poorer. UK sample had larger pores (1.00-4.00 μm) compared to R-SF9 and R-SF10 samples. Pores were highly isolated and partially eliminated but the concentration was still high. Starck sample is denser than UK sample but high concentration of small isolated pores (0.20-0.60 μm) were observed in this sample.

R-SF9 and R-SF10 samples reached almost full density at 1900°C and pores were completely eliminated in the first five minutes of the dwell period. UK sample had small pores with homogenous distribution at zero dwell and most of these were eliminated in the first 10 minutes of dwell. Results showed that the Starck powder completed significant densification at 1900°C without dwell and density was only slightly increased with extended dwell times. Intergranular pores were mostly eliminated by extended dwell time but carbon inclusions were maintained under all conditions. Some carbon inclusions were observed in all boron carbide samples even with long dwell times as seen from Figure 8. These inclusions were the results of carbon agglomerations and graphite impurities, which were carried along from the powders. Synthesized powders had a small percentage of graphitic inclusions (up to 0.2%) which may arise due to direct contamination of the graphite crucible with the RCR furnace. Given that the Starck powder had agglomerated carbon and these agglomerations likely resulted in the large carbon inclusions found in the consolidated Starck samples.

In all samples, grain sizes started to increase between 1550 and 1700°C with limited growth rate (Table 3). Grain growth rate increased after 1700°C and reached a plateau after 1900°C. Densification rate was steady among the four powders between 1550-1700°C and 1700-1850°C regimes.

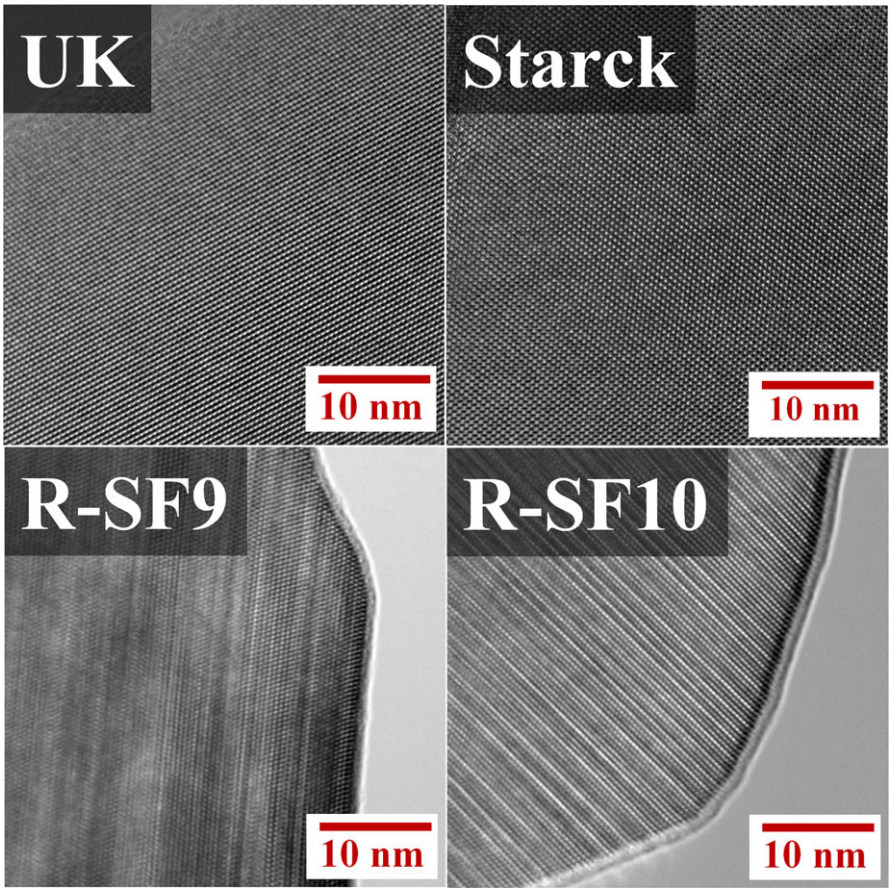

FIGURE 4 HRTEM images of RCR synthesized powders, highlighting extremely small twin spacing and surface oxide layer at the edge of particles. HRTEM images of commercial powders revealed no sign of twin. [Color figure can be viewed at wileyonlinelibrary.com]

TABLE 2 Density measurements of boron carbide samples (all results are g/cm^3)

Name	1550°C	1700°C	1850°C	1900°C	1900°C 5 min	1900°C 10 min	1900°C 20 min
R-SF9	1.56	2.06	2.47	2.49	2.51	2.51	2.51
R-SF10	1.51	2.09	2.48	2.50	2.51	2.51	2.51
UK	1.60	1.86	2.35	2.48	2.50	2.51	2.51
Starck	1.51	2.00	2.45	2.46	2.47	2.48	2.48

Densification of these powders started with pore isolation and particle rearrangement in the earlier stages of sintering. Pore elimination and closure was dominant in the later stage and this led to grain growth. Samples reached high densities at 1900°C and densification was controlled by grain boundary diffusion.

Boron carbide with smaller particle size had faster densification profile until reaching high densities (+90% TD). Carbon agglomerations in the Starck powder resulted in inclusions that prevented full density to be reached. RCR samples reached almost full density at 1900°C without dwell, whereas 5-10-minute dwell was necessary for commercial samples. The granular morphology and fine particle size led the faster densification for the RCR synthesized powder and lack of carbon inclusions helped to reach full density.

TEM analyses of dense boron carbide were performed on samples sintered at 1900°C with 10-minute dwell. UK-10 min sample had homogenous grain size in some regions. Occasionally, twins were observed in limited grains and the twin widths are usually larger than 1 μm (Figure 9). Intragranular inclusions, which are most likely from the impurities from the starting powder, were present in the dense sample. Starck-10 minute sample also had homogenous grain size distribution, but with presence of nanoscale pores. Some large grains (~5.00 μm) were observed, similar to the dense UK sample. Twins were very limited and observed in only limited grains. The twins

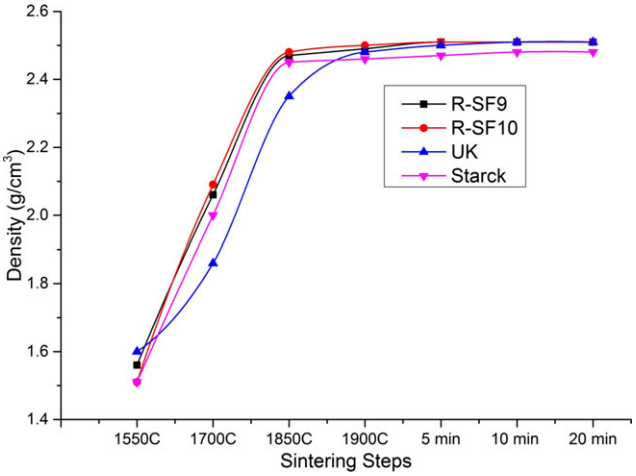

FIGURE 5 Density of boron carbide samples with various thermal treatments. [Color figure can be viewed at wileyonlinelibrary.com]

observed in dense UK and Starck samples may have originated from the limited twins found in the starting powder, or formed during the densification process. The nanoscale pores were rare in RCR samples (R-SF9 10 minute and R-SF10 10 minute samples) compared to the commercial counterparts. More interestingly, both dense RCR samples contained high twin density. Over 100 grains were checked and all grains had twins and density of twin varied from grain to grain. General observation was that smaller the grain size, higher the twin concentration. HRTEM images of R-SF9 (Figure 9) show grains with low and high twin concentration in the same sample but different grains. Distance between the planes was around 20 nm in the smaller grains and larger than 300 nm for the larger grains. Moshtaghioun et al.also showed that mean twin spacing is increased with increased grain size.[46] The twins are thought to be from the highly twinned RCR starting powders. The twin density in the densified samples decreased compared to the powders. For examples, the twins in the starting powder were only a few nanometers apart, but the ones in the dense RCR samples were tens to hundreds nanometers apart. This suggested that some reduction had occurred during the sintering process. Anselmi-Tamburini et al. observed that existed twins are eliminated during sintering process with increased temperatures.[47] Nevertheless, the dense RCR samples contain much higher twin density compared to the dense commercial samples.

3.3 | Hardness

Knoop hardness measurements were performed on each boron carbide sample sintered at 1850°C and 1900°C. Dense RCR boron carbide samples exhibited higher hardness than commercial boron carbide samples under all testing load conditions. HK_{100} results for R-dense SF9 and R-SF10 at 1850°C were higher than 31 GPa, whereas the dense commercial samples were below 29 GPa. The dense RCR samples continue to be harder than the commercial ones as the indentation load increased as shown in the Figure 10. The lower hardness of the dense UK sample may be associated with the impurities present in the final dense product. Chen et al. reported that small amount of impurities can substantially deteriorate the mechanical

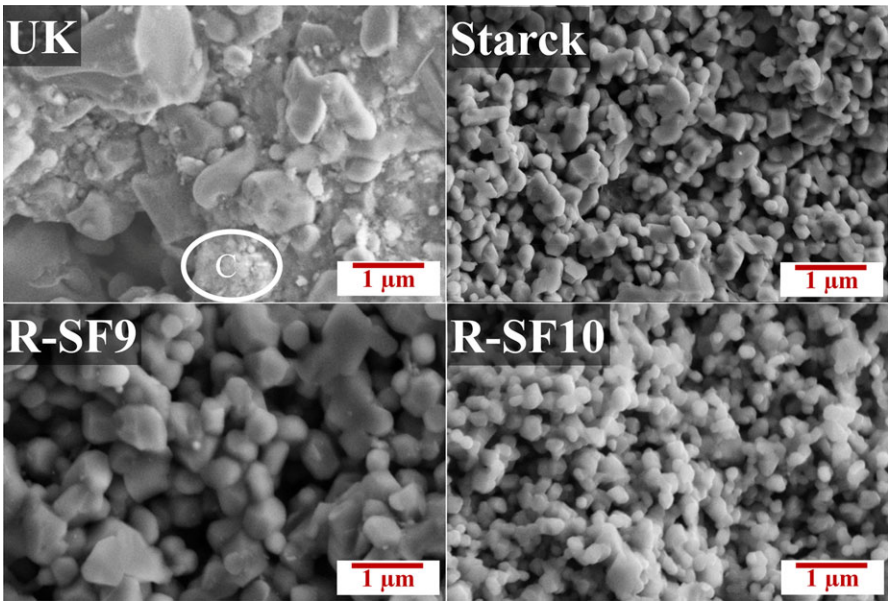

FIGURE 6 Neck formations of boron carbide compacts at 1550°C, UK sample with free carbon (encircled C) and limited neck formation, Starck and synthesized samples with neck formation in every particles. [Color figure can be viewed at wileyonlinelibrary.com]

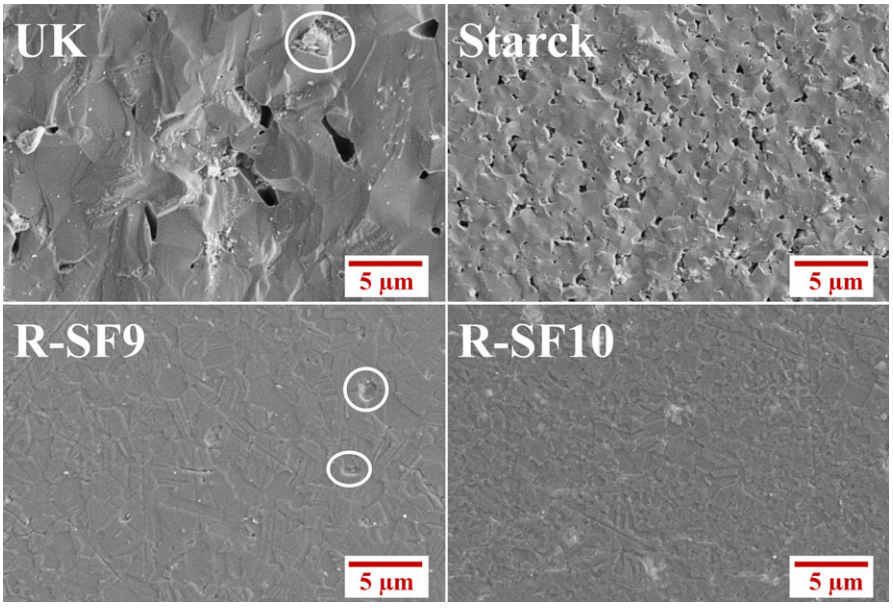

FIGURE 7 Densification of boron carbide at 1850°C, circles indicate carbon inclusions. Synthesized samples had higher densities compared to commercial samples. [Color figure can be viewed at wileyonlinelibrary.com]

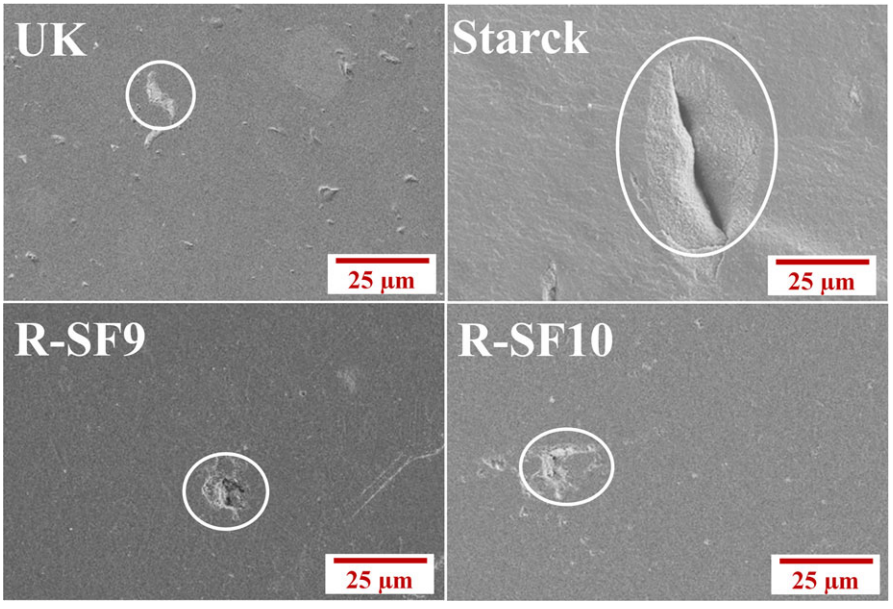

FIGURE 8 Boron carbide samples at 1900°C with 5-10-minute dwell time showing carbon inclusions. Carbon inclusions are shown in the circles. [Color figure can be viewed at wileyonlinelibrary.com]

TABLE 3 Grain size measurements of boron carbide samples (all results are μm)

Name	1550°C	1700°C	1850°C	1900°C	1900°C 5 min	1900°C 10 min	1900°C 20 min
R-SF9	0.58	0.68	1.15	1.47	1.70	1.80	1.95
R-SF10	0.20	0.38	0.69	0.79	0.96	1.39	1.65
UK	1.35	1.42	2.49	2.64	3.03	3.36	3.79
Starck	0.50	0.57	1.20	1.25	1.43	1.62	2.19

properties in boron carbide.[48] The lower hardness of the dense Starck sample may be attributed to the nanoscale pores. In addition, the carbon inclusions resulted from the high-free carbon content in the starting powder will also lower the hardness in the final consolidated products, especially under high loads.

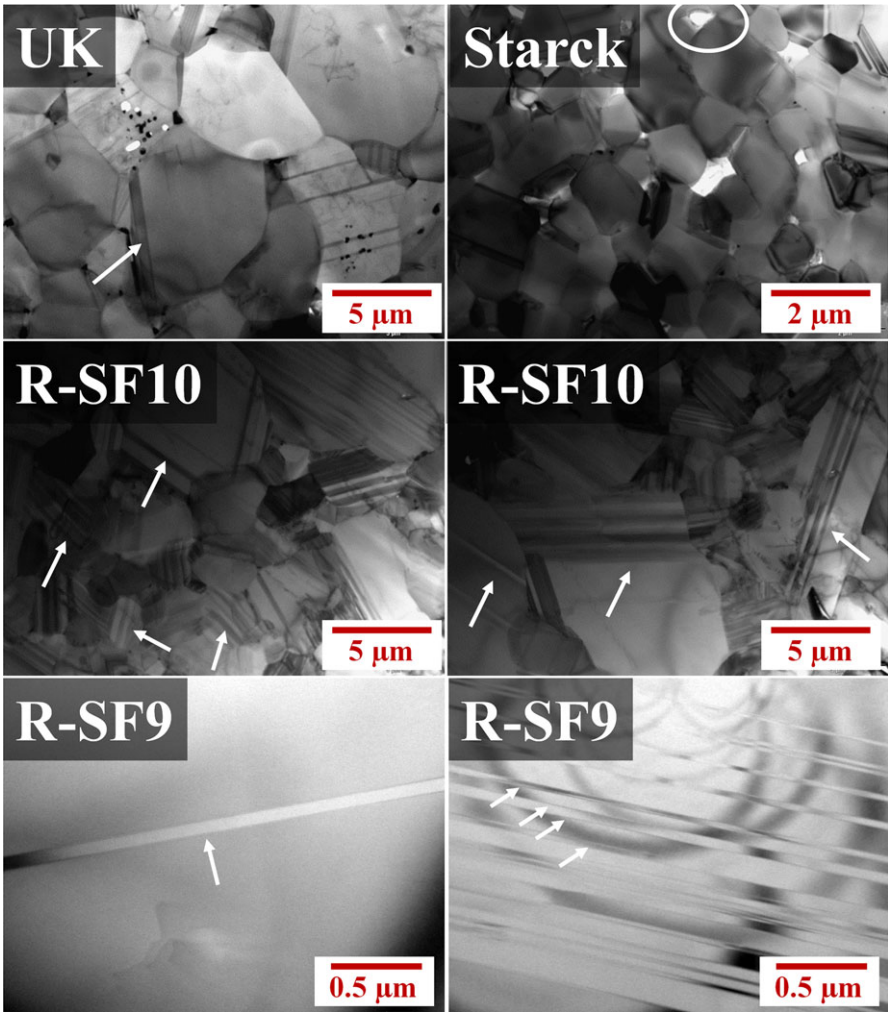

FIGURE 9 TEM images of dense boron carbide samples; UK and Starck samples with limited twins (arrows) and intragranular pores (circle). TEM images of R-SF10 sample with high and low twin concentration. HRTEM images of R-SF9 sample with low and high twins concentration. [Color figure can be viewed at wileyonlinelibrary.com]

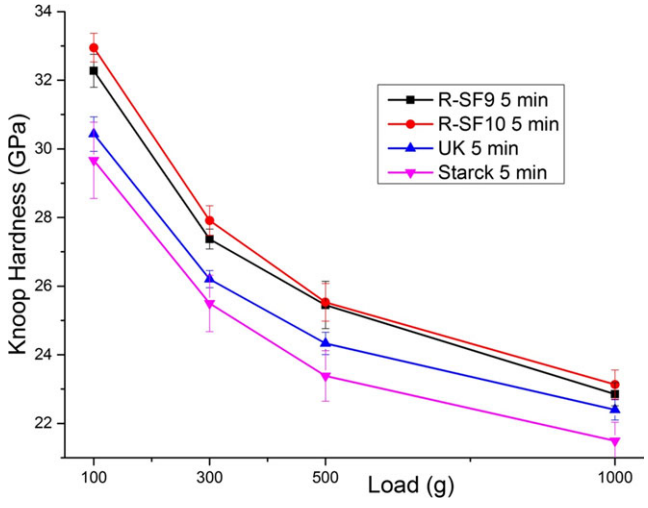

FIGURE 10 Hardness of boron carbide samples under various loads, sintered at 1900°C with five-minute dwell. [Color figure can be viewed at wileyonlinelibrary.com]

The RCR samples achieved full density without apparent impurities, carbon inclusions, and nanoscale pores, which all contribute to the improved hardness. Furthermore, high density of twins was observed in all grains. Studies of other hard materials reported that successfully synthesized nanotwinned diamond and nanotwinned cubic boron nitride displayed much higher hardness than the twin-free counterparts.[49,50] In this work, high twin concentrations (both nanoscale and submicrometer scale) were maintained during the transition from powder to dense RCR boron carbide final products. A combination of lower percentages of second phases as well as the presence of high density of twins led to the high hardness in the dense RCR samples.

4 | CONCLUSIONS

Boron carbide powders with reduced free carbon were successfully synthesized by RCR. The RCR powders are

submicrometer in size and contain extremely high density of twins compared to the commercial powders. Dense sample fabricated from the RCR powders had limited grain growth and maintained the high twin density. Moreover, the RCR samples densified better than the commercial samples, which may be attributed to the fine grain size and equiaxed granular morphology. The dense RCR samples also exhibited higher hardness. The improved mechanical property is likely a combinatory effect of excellent densification, low-free carbon content, and high twin density.

ACKNOWLEDGMENTS

This research was sponsored by the Army Research Laboratory and was accomplished under Cooperative Agreement W911NF-12-2-0022. Additional support was received from the Defense Advanced Research Projects Agency W31P4Q-13-1-0001 and from the National Science Foundation I/UCRC Award No. 1540027.

REFERENCES

1. Vogler TJ, Reinhart WD, Chhabildas LC. Dynamic behavior of boron carbide. *J Appl Phys*. 2004;95:4173–4183.
2. Zeng Y, Feng J, Ding C. Microstructure and properties of plasma spraying boron carbide coating. *J Mater Sci Technol*. 2000;16:63–66.
3. Hollenberg GW, Walther G. The elastic modulus and fracture of boron carbide. *J Am Ceram Soc*. 1980;63:610–613.
4. Lee H, Speyer RF. Hardness and fracture toughness of pressureless-sintered boron carbide (B4C). *J Am Ceram Soc*. 2002;85:1291–1293.
5. Thevenot F. Boron carbide- a comprehensive review. *J Eur Ceram Soc*. 1990;6:205–225.
6. Champagne B, Angers R. Mechanical properties of hot pressed B-B4C materials. *J Am Ceram Soc*. 1979;62:149–153.
7. Barick P, Jana DC, Thiyagarajan N. Effect of particle size on the mechanical properties of reaction bonded boron carbide ceramics. *Ceram Int*. 2013;39:763–770.
8. Krell A. A new look at grain size and load effects in the hardness of ceramics. *Mater Sci Eng, A*. 1998;245:277–284.
9. Reddy KM, Guo JJ, Shinoda Y, et al. Enhanced mechanical properties of nanocrystalline boron carbide by nanoporosity and interface phases. *Nat Commun*. 2012;3:1052.
10. Niihara K, Nakahira A, Hirai T. The effect of stoichiometry on mechanical properties of boron carbide. *J Am Ceram Soc*. 1984;67:C13–C14.
11. Domnich V, Reynaud S, Haber RA, Chhowalla M. Boron carbide: structure, properties, and stability under stress. *J Am Ceram Soc*. 2011;94:3605–3628.
12. Lipp A. *Boron Carbide: Production, Properties, Application*. Elektroschmelzwerk Kempten GmbH, Munich, 1966.
13. Wilson WS and Guichelaar PJ. Electric arc furnace processes. In: Weimer A, ed. *Carbide, Nitride and Boride Materials Synthesis and Processing*. Dordrecht: Springer Netherlands; 1997:131–136.
14. Thévenot F. Industrial preparation of Boron–Carbide Powders. In: Zuckerman JJ, Hagen AP, eds. *Inorganic Reactions and Methods: The Formation of Bonds to C, Si, Ge, Sn, Pb (Part 2), Volume 10*. Hoboken, NJ: John Wiley & Sons, Inc.; 1989:3–4.
15. Chheda M, Shih J, Gump C, Weimer AW. *Synthesis and Processing of Boron-Rich Boron Carbide*, 2008.
16. Suri AK, Subramanian C, Sonber JK, Murthy TSRC. Synthesis and consolidation of boron carbide: a review. *Int Mater Rev*. 2010;55:4–40.
17. Alizadeh A, Taheri-Nassaj E, Ehsani N. Synthesis of boron carbide powder by a carbothermic reduction process. *J Eur Ceram Soc*. 2004;24:3227–3234.
18. Goller G, Toy C, Tekin A, Gupta CK. The production of boron carbide by carbothermic reduction. *High Temp Mater Process*. 1996;15:117–122.
19. Weimer AW, Roach RP, Haney CN, Moore WG, Rafaniello W. Rapid carbothermal reduction of boron oxide in a graphite transport reactor. *AIChE J*. 1991;37:759–768.
20. Rafaniello W, Moore WG. *Producing boron carbide*, [4,804,525], 1989.
21. Weimer AW, Moore WG, Roach RP, Hitt JE, Dixit RS, Pratsinis SE. Kinetics of carbothermal reduction synthesis of boron carbide. *J Am Ceram Soc*. 1992;75:2509–2514.
22. Kalandadze GI, Shalamberidze SO, Peikrishvili AB. Sintering of boron and boron carbide. *J Solid State Chem*. 2000;154:194–198.
23. Zhang M, Zhang WK, Gao LZ, Zhang YJ. Fabrication and microstructure of B4C matrix composites by hot-pressing sinter. *Advenced Mater Res*. 2011;368:326–329.
24. Liu CH. Structure and properties of boron carbide with aluminum incorporation. *Mater Sci Eng B-Solid State Mater Adv Technol*. 2000;72:23–26.
25. Xie KY, Toksoy MF, Kuwelkar K, et al. Effect of alumina on the structure and mechanical properties of spark plasma sintered boron carbide. *J Am Ceram Soc*. 2014;97:3710–3718.
26. Skorokhod VV, Krstic VD. Processing, microstructure, and mechanical properties of B4C-TiB2 particulate sintered composites. II. Fracture and mechanical properties. *Powder Metall Met Ceram*. 2000;39:504–513.
27. Hirota K, Nakayama Y, Nakane S. Boron Carbide Ceramic and Manufacturing Method Thereof; 2011.
28. Lee CH, Kim CH. Pressureless sintering and related reaction phenomena of Al2O3-doped B4C. *J Mater Sci*. 1992;27:6335–6340.
29. Angers R, Beauvy M. Hot-pressing of boron carbide. *Ceram Int*. 1984;10:49–55.
30. Ruh R, Kearns M, Zangvil A, Xu Y. Phase and property studies of boron carbide-boron nitride composites. *J Am Ceram Soc*. 1992;75:864–872.
31. Osipov AD, Ostapenko IT, Slezov VV, Tarasov RV, Podtykan VP, Kartsev NF. Effect of porosity and grain size on the mechanical properties of hot-pressed boron carbide. *Powder Metall Met Ceram*. 1982;21:55–58.
32. Jianxin D. Erosion wear of boron carbide ceramic nozzles by abrasive air-jets. *Mater Sci Eng, A*. 2005;408:227–233.
33. Groza JR, Zavaliangos A. Sintering activation by external electrical field. *Mater Sci Eng, A*. 2000;287:171–177.
34. Saheb N, Iqbal Z, Khalil A, et al. Spark plasma sintering of metals and metal matrix nanocomposites: a review. *J Nanomater*. 2012;2012:1–13.
35. Maitre A, Vande Put A, Laval JP, Valette S, Trolliard G. Role of boron on the Spark Plasma Sintering of an alpha-*SiC* powder. *J Eur Ceram Soc*. 2008;28:1881–1890.

36. Hulbert DM, Jiang D, Dudina DV, Mukherjee AK. The synthesis and consolidation of hard materials by spark plasma sintering. *Int J Refract Met Hard Mater*. 2009;27:367–375.
37. Munir Z, Anselmi-Tamburini U, Ohyanagi M. The effect of electric field and pressure on the synthesis and consolidation of materials: a review of the spark plasma sintering method. *J Mater Sci*. 2006;41:763–777.
38. Hayun S, Weizmann A, Dariel MP, Frage N. Microstructural evolution during the infiltration of boron carbide with molten silicon. *J Eur Ceram Soc*. 2010;30:1007–1014.
39. Li X, Jiang D, Zhang J, Lin Q, Chen Z, Huang Z. Densification behavior and related phenomena of spark plasma sintered boron carbide. *Ceram Int*. 2013;40:4359–4366.
40. Sairam K, Sonber JK, Murthy TSRC, et al. Influence of spark plasma sintering parameters on densification and mechanical properties of boron carbide. *Int J Refract Met Hard Mater*. 2014; 42:185–192.
41. Moshtaghioun BM, Cumbrera-Hernández F, Gómez-García D, et al. Effect of spark plasma sintering parameters on microstructure and room-temperature hardness and toughness of fine-grained boron carbide (B4C). *J Eur Ceram Soc*. 2013;33:361–369.
42. Ji W, Rehman SS, Wang W, et al. Sintering boron carbide ceramics without grain growth by plastic deformation as the dominant densification mechanism. *Sci Rep*. 2015;5:15827.
43. Kuwelkar K, Domnich V, Haber RA. Assessing the Carbon Concentration in Boron Carbide: A Combined X-Ray Diffraction and Chemical Analysis. In: LaSalvia JC, ed. *Advances In Ceramic Armor X: A Collection Of Papers Presented At The 38th International Conference On Advanced Ceramics And Composites January 27–31, 2014*. Hoboken, NJ: John Wiley & Sons, Inc.; 2014:103–109.
44. Aselage TL, Tissot RG. Lattice Constants of Boron Carbide. *J Am Ceram Soc*. 1992;75:2207–2212.
45. Xie KY, An Q, Toksoy MF, et al. Atomic-level understanding of 'Asymmetric Twins' in boron carbide. *Phys Rev Lett*. 2015;115:175501.
46. Moshtaghioun BM, Gomez-Garcia D, Dominguez-Rodriguez A, Todd RI. Grain size dependence of hardness and fracture toughness in pure near fully-dense boron carbide ceramics. *J Eur Ceram Soc*. 2016;36:1829–1834.
47. Anselmi-Tamburini U, Munir ZA, Kodera Y, Imai T, Ohyanagi M. Influence of synthesis temperature on the defect structure of boron carbide: experimental and modeling studies. *J Am Ceram Soc*. 2005;88:1382–1387.
48. Chen MW, McCauley JW, LaSalvia JC, Hemker KJ. Microstructural characterization of hot-pressed boron carbide ceramics. *J Am Ceram Soc*. 2005;88:1935–1942.
49. Tian Y, Xu B, Yu D, et al. Ultrahard nanotwinned cubic boron nitride. *Nature*. 2013;493:385–388.
50. Huang Q, Yu D, Xu B, et al. Nanotwinned diamond with unprecedented hardness and stability. *Nature*. 2014;510:250–253.

How to cite this article: Toksoy MF, Rafaniello W, Xie K, Ma L, Hemker K, Haber R. Densification and characterization of rapid carbothermal synthesized boron carbide. *Int J Appl Ceram Technol*. 2017; 14:443–453.